Computational Drug Design of Novel Small Molecule Inhibitors for Therapy in Pancreatic Ductal Adenocarcinoma

Aryansh Shrivastava[1]
[1]Washington High School, Fremont, CA

1. Abstract

Today, pancreatic ductal adenocarcinoma, the most common form of pancreatic cancer, is one of the deadliest cancer types and remains largely unresolved. Through my research, I engineer a class of novel small molecule ligands to cure the disease by inhibiting its central carcinogenic pathway, taking the unique approach of applying the framework of targeted drug therapy and leveraging computer-aided techniques.

The target molecule for which drug design is employed is xCT, a protein embedded in the ductal cell membrane that enables cancer cells to survive without a nutrient supply and kills normal cells of the pancreas. All viable drug candidate ligands must be engineered to have a complementary structure and biochemistry to the binding site of xCT.

Starting with some known ligands of xCT to first identify the binding site and binding mode, I conduct guided substituent recombination based on the analysis of hydrophobicity and Coulombic surfaces as well as intermolecular interactions through computational docking simulations. In doing so, I employ industry-grade softwares including Chimera (to visualize 3D structures), Avogadro (to minimize free energies and infer 3D chemical structures), ChemDraw (to draw 2D chemical structures), AutoDockTools (to visualize the location of the binding site), AutoDock Vina (to perform docking simulations), and the SeaWulf computational cluster (for intensive, high accuracy computations).

A total of 1461 novel results are tabulated, and the top two drug candidates among them are found to be CID 136204070 and 135564873, the best one among them CID 135564873. These can be used by drug industries to create new targeted drug therapies for pancreatic cancer, increasing the survival rate of the disease and saving countless lives through proactive treatment despite diagnostic delays. I've computationally ensured the absorption, distribution, metabolism, excretion, and toxicity results for the final drug candidates, and all of the relevant quantities are computationally verified through well-defined biochemistry lab procedures for the final ligand molecules and found to be very reliable for drug candidacy.

I did this project through the Simons Summer Research Program at Stony Brook University as a Simons Fellow and paid research intern, under the guidance of Distinguished Professor Iwao Ojima and student mentors Adam Taouil and Frank Wang. I’m also in the process of discussing publishing this research with Distinguished Professor Iwao Ojima to share my research with the community.

2. Background

2.1. Background: Targeted Drug Therapy

In recent years, targeted drug therapy has emerged as a method to treat cancers whereby a molecule can be engineered into a drug and delivered to the target site of a disease within the human body to prevent its growth and progression. In particular, our bodies' metabolic processes are large networks of pathways that relay signals across chains of molecules, each specialized to perform a certain task, and cancers proliferate by hijacking these conventional pathways to form alternate, carcinogenic pathways involving different proteins or expression levels with eventually detrimental macroscopic symptoms, such as the fatal inflammations we call tumors. However, the delivery of molecules to intercept these alternate pathways by inhibiting the functions of key intermediary molecules allows for the natural prevention of diseases, as detailed below.

Structurally, the delivered molecules are known as ligands, as they bind to the intermediary molecules at one or more binding sites to prevent their function by blocking their structure. Therapeutically, they are also known as drugs (or drug candidates), as they are intended to treat patients of detrimental cancer-related symptoms.

Binding affinity is the term used for the strength and effectiveness of the binding mode of a ligand to an intermediary molecule in a carcinogenic pathway. To best block the intermediary molecules and be effective as drugs, ligands must therefore exhibit high binding affinity. In general, the higher the binding affinity, the more effective the ligand is as a drug. In order for developed ligands to have a high binding affinity, they must be complementary in both shape and electrochemistry to the intermediary molecule at the binding site of interest. It is rare for two different types of intermediary molecules to have the same structure and electrochemistry, so any given ligand must be engineered according to exactly one type of intermediary molecule, known as the target molecule. This is the main appeal of targeted drug therapy—with very specific target molecules, unintended side-effects, such as binding to a different molecule, can be prevented.

The three forms of targeted drug therapy are shown below. Out of these, the ideal form of targeted drug therapy is creating a small molecule ligand to inhibit a particular target protein, as reasoned below.

Three Forms of Targeted Drug Therapy

Small molecule ligand and small molecule target	Small molecule ligand and protein target	Protein ligand and protein target
Not ideal—small molecule targets tend to have very few binding pockets and may require significant structural disruptions to inhibit function	Ideal—protein targets usually have multiple possible binding pockets, and even small structural disruptions in proteins can cause them to	Not ideal—protein-protein interactions are very complex and often unpredictable (complex structure and dynamics of each individual

	become dysfunctional	protein combining together)

2.2 Background: Computer-Aided Drug Design

To utilize this framework of ideal targeted drug therapy (a small molecule targeting a protein) in drug development, I can turn to computer-aided drug design. In particular, I can specify a 3D sample space containing a binding site on the structure of the target protein (usually a binding pocket that indents the surrounding structure) and try a spectrum of different orientations of a particular ligand to find the best one. This procedure is called docking.

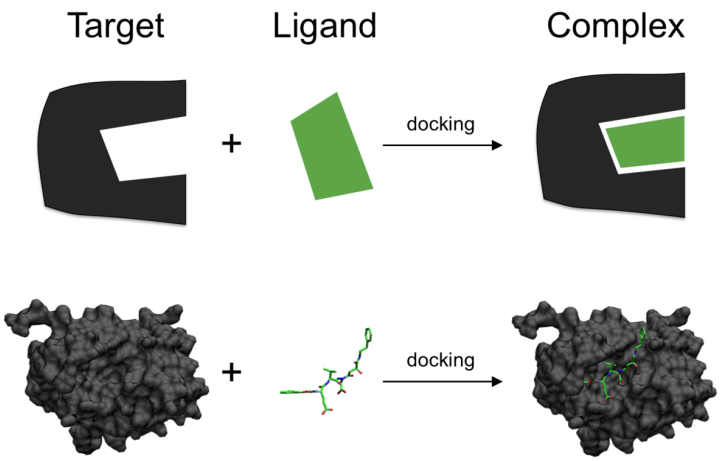

Figure 1. An illustration of what it means to dock a ligand on a target molecule. As illustrated, the ligand must have complementary structure and electrochemistry to that of the target molecule at the binding site. Copied from (*1*).

To simulate ligand binding, via a computer program, I can build overlapping force fields based on the structure and electrochemistry of the amino acids (also known as residues) in the target protein, attracting or repelling different substituents (structural parts) of the ligand. A value called the free energy of binding, with units of kcal/mol, can be ascribed to the resulting system of force fields as a measure of the total potential energy, which indicates how spontaneously the system causes the ligand to bind to the protein at these particular residues. When this free energy of binding is negative, there is a spontaneous attraction between substituents of the ligand to parts of the binding pocket, and, the greater its absolute value, the more spontaneous the reaction. This means that the free energy of binding is in fact one measure for the binding affinity of a ligand with respect to a particular binding pocket.

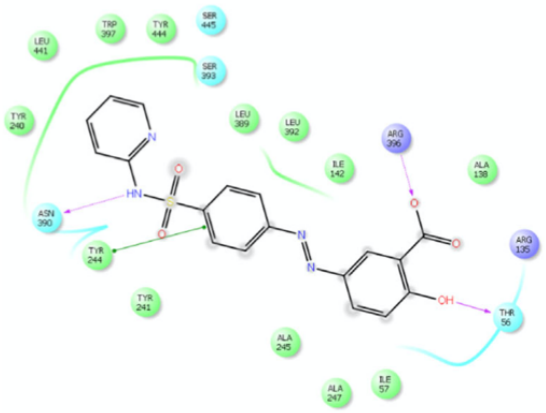

Figure 2. Overlapping force fields stemming from the structure and electrochemistry of surrounding amino acid residues in the binding pocket attract or repel various chemical substituents of a ligand, creating a free energy of binding that determines the strength of the binding mode. Copied from (*2*).

3. Introduction

3.1. Introduction: Pancreatic Ductal Adenocarcinoma

Over 90% of all malignancies associated with pancreatic cancer are pancreatic ductal adenocarcinomas (PDAC), which have a 5-year survival rate of only 10%, the lowest among all cancer types. Thus far, no mechanisms for early diagnosis exist—there are no peripheral biomarkers to gauge initial tumor growth, and symptoms occur only in later stages—so PDAC has a very poor prognosis among patients and often leads to fatality (*3*).

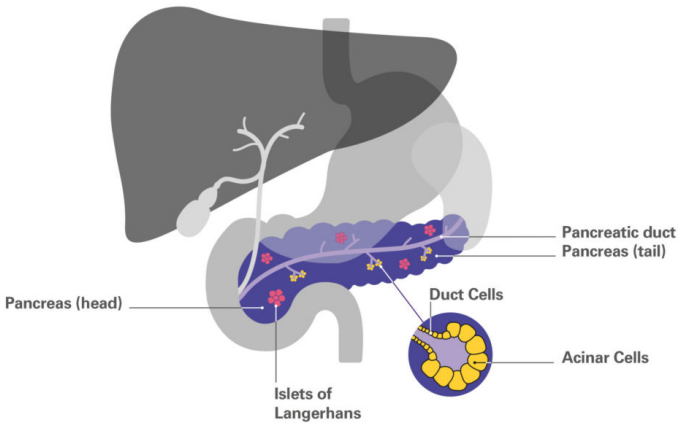

Figure 3. Pancreatic ductal adenocarcinoma (PDAC) originates in the duct cells of the pancreas, as depicted. Copied from (*4*).

A major hallmark of interest in PDAC is the dense fibrous connective tissue of cancer-associated fibroblasts (CAF) that constitutes over 90% of the tumor by volume, causing hypoxia, a lack of oxygen that elicits oxidative stress, and nutrient deprivation in the microenvironment. These conditions are known to kill normal cells of the pancreas while transitioning epithelial (surface) cancer cells into a mesenchymal (connective fibrotic) phenotype with a greater metastatic and fibrotic potential (*3*). In this way, fibrosis induces itself in a positive feedback loop. The fatality of PDAC can be attributed to this accelerated metastasis and fibrosis: they drive the progression to later stages.

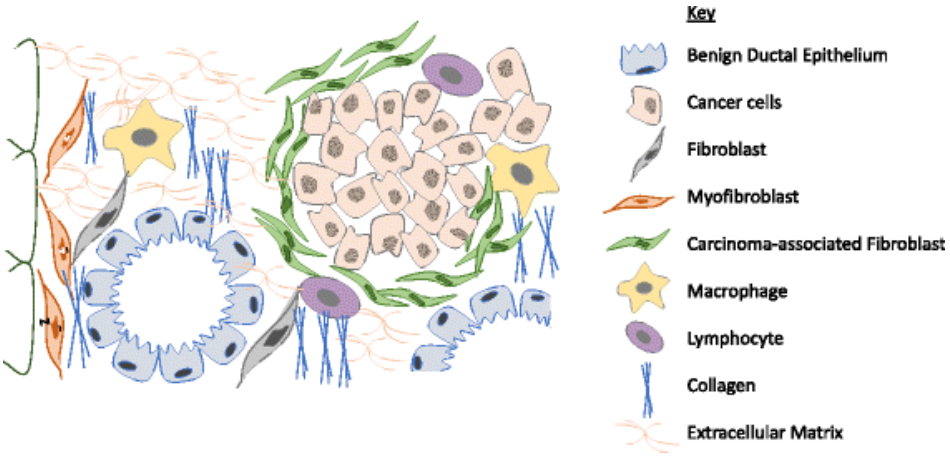

Figure 4. The CAF-bound PDAC microenvironment. Adapted from (*5*).

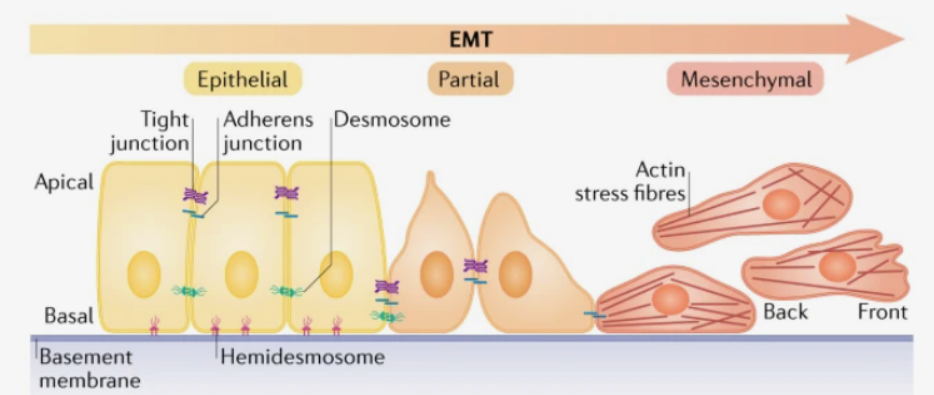

Figure 5. The process of epithelial to mesenchymal transition in fibrosis. Adapted from (*6*).

While conventional drug therapies attempt to target PDAC tumors directly, their cells are already shielded by layers of fibroblasts due to late diagnosis, hindering the distribution of the drug in the body. In stark contrast, I propose a unique therapeutic strategy involving the pathological interception of the feedback loop to halt fibrosis, eliminating all developed tumor sites.

3.2. Introduction: xCT

Pathologically, in the process of fibrosis, xCT (SLC7A11) is one of the most critical carcinogenic proteins, an integral membrane cotransporter embedded in PDAC cell membranes that releases the amino acid glutamate out of the cell in exchange for the transfer of cystine into the cell. This cystine is then reduced to cysteine, key to both the synthesis of disulfide bonds in CAFs and numerous antioxidant biomolecules, especially the protein glutathione (GSH), which alters tumor cell metabolism to survive the otherwise lethal conditions in the microenvironment by suppressing the ferroptotic tendency toward cell death (*7*). As such, epithelial tumor cells as well as mesenchymal connective CAF cells overexpress xCT for a very high cysteine influx as a means to survive and metastasize.

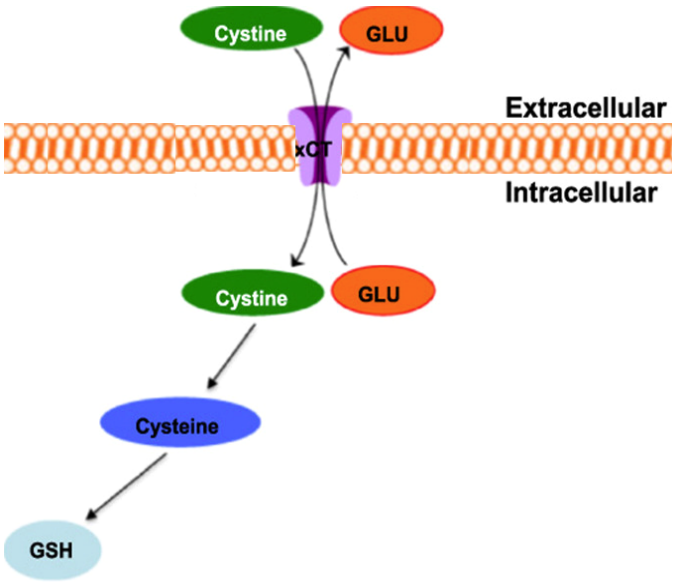

Figure 6. The xCT-mediated GSH proliferation pathway. Adapted from (*8*).

Inhibition of xCT by engineering a small molecule will greatly decrease cysteine influx, disrupting the positive feedback loop of fibrosis and preventing PDAC metastasis— cystine is too polar and lipophobic to dissolve into the cell membrane's phospholipid bilayer directly. Because there will no longer be sufficient cysteine supplied by functioning xCT for the synthesis of GSH, upon depletion of its supply in the microenvironment, all tumor sites will die of ferroptosis. However, healthy cells, not reliant on xCT overexpression, will survive.

Overall, the primary aim is to computationally design and evaluate a novel class of high affinity small molecule inhibitors for xCT to treat PDAC despite diagnostic delay.

4. Methods

4.1. Methods: Setup

xCT has several known small molecule inhibitor ligands including sulfasalazine (SFZ), sorafenib (SB), and erastin (ER), along with a crystal structure readily available in the PDB (*9, 10*).

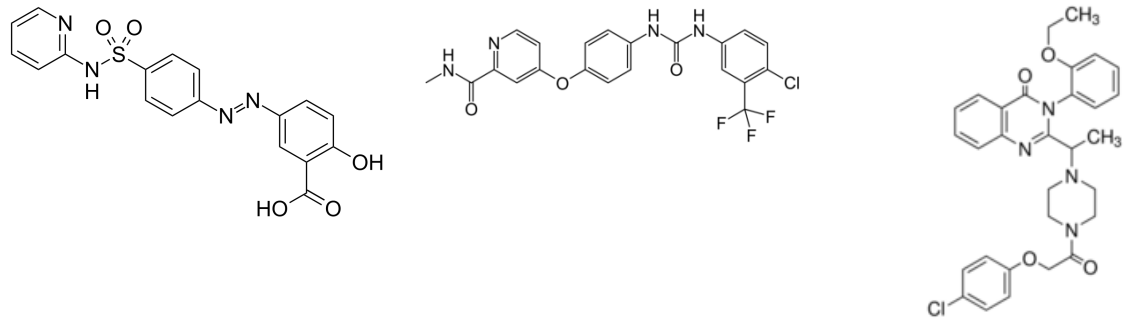

Figure 7. From left to right, the 2D chemical structures of the ligands SFZ, SB, and ER.

Therefore, structure-based drug design—designing a ligand based on a target with known structure—is an ideal methodology to follow for xCT.

4.2. Methods: Docking Preparation

Throughout the design process, candidate inhibitor designs must be docked and scored. Before this, however, the protein and ligand structures must be prepared for docking.

First, hydrogens are added to the PDB structures of the protein and each of the ligands in Chimera according to standard rules for stable chemical structure (valence rules, minimization of formal charges, etc.). This is because the technique utilized to create the PDB structures is X-ray diffraction, which relies on observing the diffraction trajectories of X-rays off of electrons, yet hydrogen has an electron density of almost zero, so it goes mostly undetected.

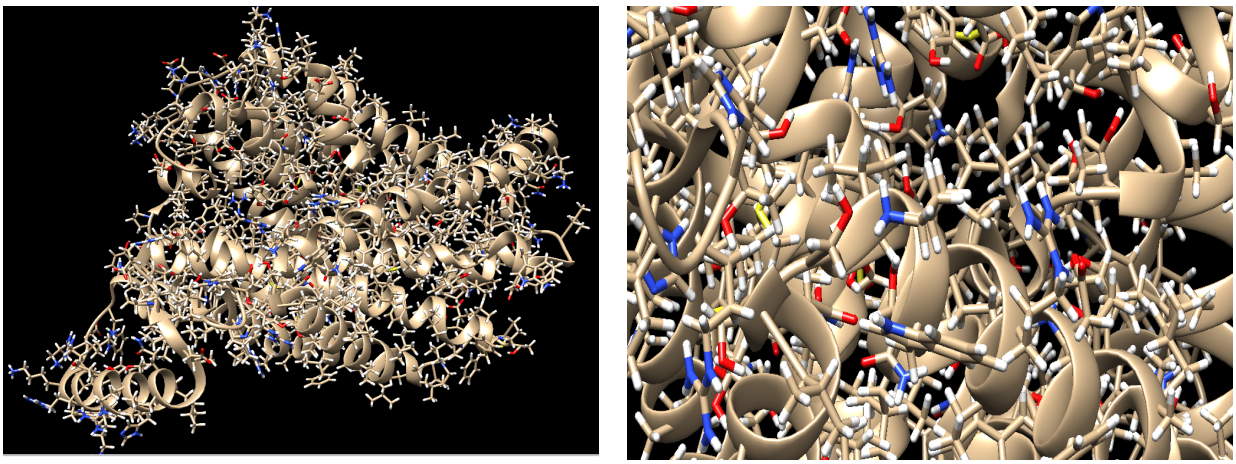

Figure 8. The addition of hydrogens on the structure of xCT. On the left is an overlay of the ribbon structure and the ball-and-stick structure for the protein. Elements are colored according to the CPK standard, so white denotes hydrogen, which can be found in the closeup on the right.

Second, the free energy for the PDB structures of the protein and each of the ligands is minimized according to the MMFF94 force field in Avogadro to best approximate the bioactive conformation of the molecules. To elaborate, in chemical physics systems, all chemical bonds and interactions can be considered springs. Chemical bonds and interactions, like springs, always naturally tend toward the state of least potential energy, so this energy minimization step refines that aspect of the computational simulation.

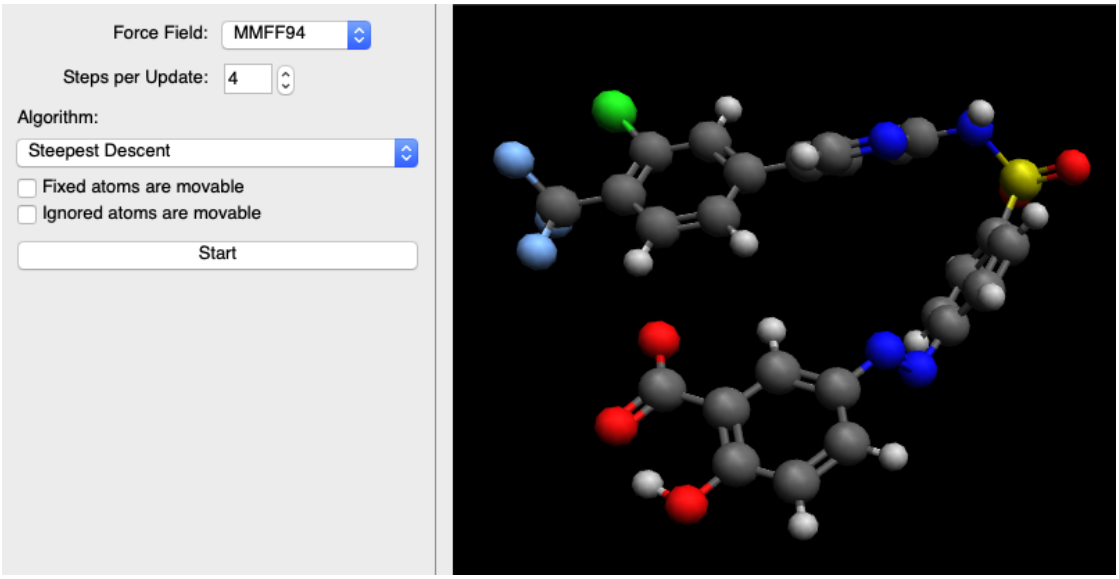

Figure 9. Energy minimization of the 3D structure of the SFZ ligand in Avogadro based on the MMFF94 force field and steepest descent.

Third, the nonpolar hydrogens in the PDB structures of the ligands are merged using either AutoDockTools or a Python script (where the latter is convenient for large-scale operations). This merging will greatly reduce the computational intensity of docking without sacrificing accuracy because nonpolar hydrogens contribute very little to the overall structure and electrochemistry of a ligand.

```
i aryansh % python scripts/prepare_ligand4.py -l sfz1.mol2
```

```
if charges_to_add is not None:
    #restore any previous charges
    for atom, chargeList in preserved.items():
        atom._charges[chargeList[0]] = chargeList[1]
        atom.chargeSet = chargeList[0]
if verbose: print "returning ", mol.returnCode
bad_list = []
for a in mol.allAtoms:
    if a in coord_dict.keys() and a.coords!=coord_dict[a]:
        bad_list.append(a)
if len(bad_list):
    print len(bad_list), ' atom coordinates changed!'
    for a in bad_list:
        print a.name, ":", coord_dict[a], ' -> ', a.coords
else:
    if verbose: print "No change in atomic coordinates"
if mol.returnCode!=0:
    sys.stderr.write(mol.returnMsg+"\n")
sys.exit(mol.returnCode)
```

Figure 10. Python terminal command for merging nonpolar hydrogens in the energy-minimized sfz1.mol2 ligand file using the script prepare_ligand4.py. The relevant excerpt of the script file, responsible for merging the hydrogens, is included.

4.3. Methods: Docking Simulations

After these preparation steps, computer-aided molecular dynamics simulations to find the top configurations of a small molecule ligand ranked based on the binding energy, also known as docking simulations, can be done using AutoDock Vina, a popular open source docking program. Because of the numerous electrochemical effects, it is impossible to predict the exact free energy of binding for a particular configuration, so AutoDock Vina calculates its own binding energy score using the Vinardo function. With the Vinardo function, an improvement of -1.4 kcal/mol corresponds to a 10-fold increase in true affinity of a ligand to a protein (defined by a quantity called the equilibrium association constant), so it will be essential to keep track of this binding score when I commence with ligand engineering.

Also, in true biological systems, all molecules including proteins are very flexible and constantly change their conformations. However, brute force accounting for this flexibility is not only very time consuming but often inaccurate due to compromises made for each individual conformation. Therefore, instead of using flexible docking, I will use rigid docking, keeping both the protein and the ligand fixed in their most likely bioactive (true biological) conformations.

All prepared files for the protein and ligand are given to Vina for rigid docking along with the center and dimensions of a grid box specifying the location of the target binding site to calculate the most probable binding pose.

4.4. Methods: Other Affinity Metrics

Once the most probable binding pose is calculated for each ligand, it can be used to compare between ligands by affinity to see which ligand makes the best drug candidate. It is important to note, however, that Vina's binding energy score alone may not be sufficient to determine the most probable ligand binding pose, or even the affinity. For instance, approximation errors in the Vinardo function or other assumptions made in the docking process may come into account for deviations in binding scores within around 1 kcal/mol of one another, and it cannot be ascertained that the score with the greatest absolute value is the best among them.

As such, instead of relying on Vina's energy score alone to compare affinity between ligands within 1 kcal/mol of one another, I can also integrate computational comparisons of the intermolecular attractions (such as hydrogen bonding and interactions), spatial orientations (e.g., ensuring concavities in protein structure typically align with convexities in ligand structure), and hydrophobicity and Coulombic surfaces.

It is important to note that, among all intermolecular attractions, hydrogen bonding is generally the strongest, so the number of hydrogen bonds to residues in a binding pocket can provide a decent first order approximation of affinity to differentiate binding scores close to one another. However, on the second order, it is also beneficial to consider the number of contacts and clashes between the Van der Waals radii of adjacent atoms—a large number of contacts in one area of the pocket may produce a total attraction that classifies on the first order, while a large number of clashes may similarly produce a first-order repulsion.

The hydrophobicity surface of the protein will unveil which subunits are hydrophilic (equivalently, lipophobic), colored blue, and which are hydrophobic (equivalently, lipophilic), colored red. Based on this, I know to engineer ligand substituents near hydrophilic protein subunits to be hydrophilic, and ligand substituents near hydrophobic protein subunits to be hydrophobic.

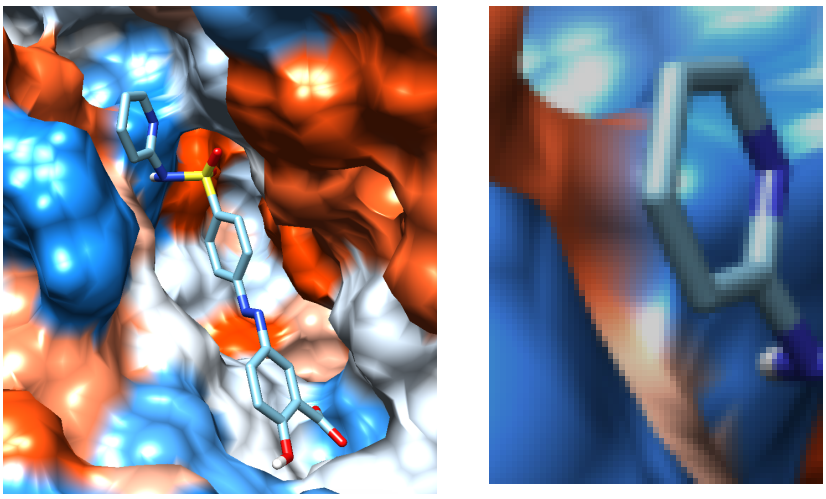

Figure 11. An example of what a hydrophobic surface looks like. In this example, the hydrophilic hydrogen atom complements the hydrophilic (blue) part of the binding pocket it angles toward.

The Coulombic surface of the protein will unveil which subunits have positive electrostatic surface potential (meaning they attract δ- atoms), colored blue, and which subunits have negative electrostatic surface potential (meaning they attract δ+ atoms), colored red. Based on this, I know to engineer ligand bonds near positive electrostatic surface potential protein subunits to have the more electronegative atom (δ-) near the subunit surface, and ligand bonds near negative electrostatic surface potential protein subunits to have the more electropositive atom (δ+) near the subunit surface.

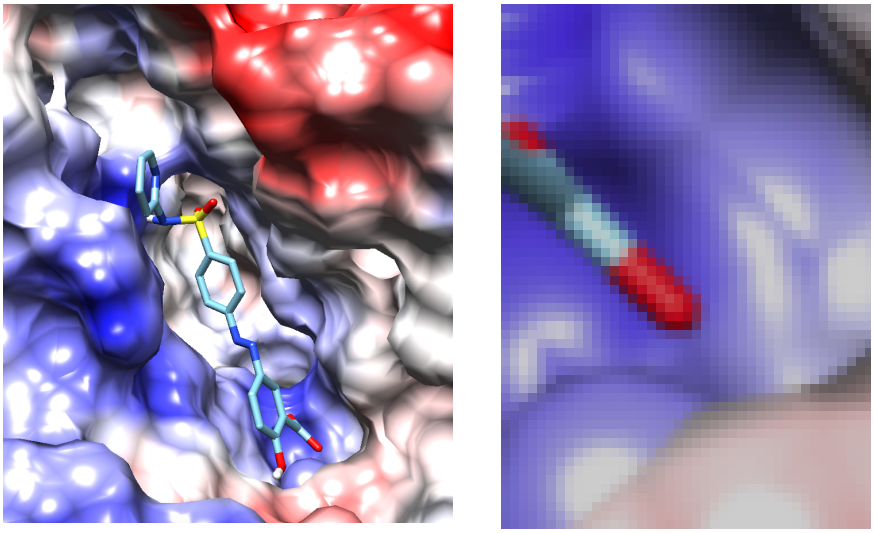

Figure 12. An example of what a Coulombic surface looks like. In this example, the nitrogen atom in the carbon-nitrogen bond accumulates a δ- charge charge, complementing the positive electrostatic surface potential (blue) of the binding pocket.

4.5. Methods: SFZ Validation

Foremost, it is necessary to validate the protein with a ligand to reproduce a known binding pose as a baseline. This will tell us the location of a feasible binding pocket on the surface of the protein as well as the approximate spatial orientation I should expect in docking.

It would be preferable for validation if a ligand came as a co-crystal (that is, already embedded in the structure of the protein, with an exactly known fit), but the sole crystal structure for xCT in the PDB does not include a ligand as a co-crystal. However, the structure is human-derived, in a complex with CD98hc (another supporting protein of the xc- system), so it can be still used for validation in conjunction with the crystal structure of a known ligand and some information regarding its binding interaction (*11*). Of the three ligands identified, SFZ is the most appealing as a hit ligand: not only does it have the least molar mass and simplest chemical structure, but it is also the only one with homology models of its binding interaction with xCT based on another amino acid transporter protein, ApCT (*10*). (A homology model is a 3D structure derived by comparison of the tertiary and quaternary structure of a given protein-ligand interaction to that of the interaction of the ligand with a related protein whose structure is known. In this case, even though the xCT-SFZ complex could not be directly constructed with X-ray crystallography, it could be inferred based on the creation of a homology model with the ApCT-SFZ complex.)

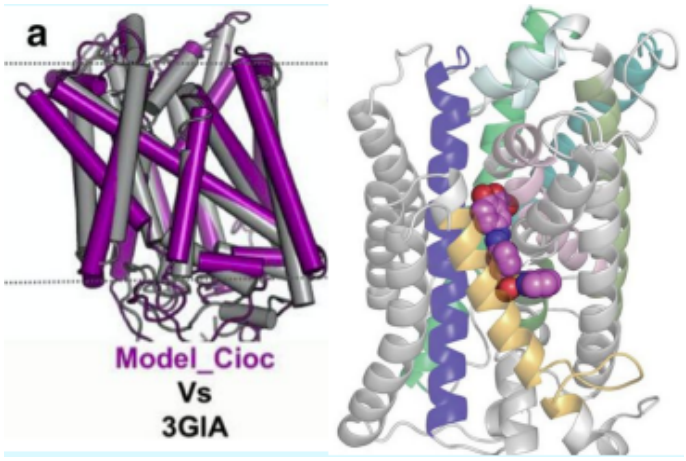

Figure 13. An overlay of the homology model for xCT atop the structure of ApCT (3GIA), and the predicted binding mode of SFZ with xCT based on this homology model (right). Adapted from (*10*).

In initial validation, SFZ was docked into the binding pocket surrounded by the amino acid residues mentioned in the homology model in the protein structure of xCT, with an optimal

binding score of -9.3 kcal/mol calculated by Vina and visualized on Chimera, where, as mentioned earlier, the negative sign denotes the spontaneity of binding, and this docking matched the homology model in terms of the surrounding helices and residues.

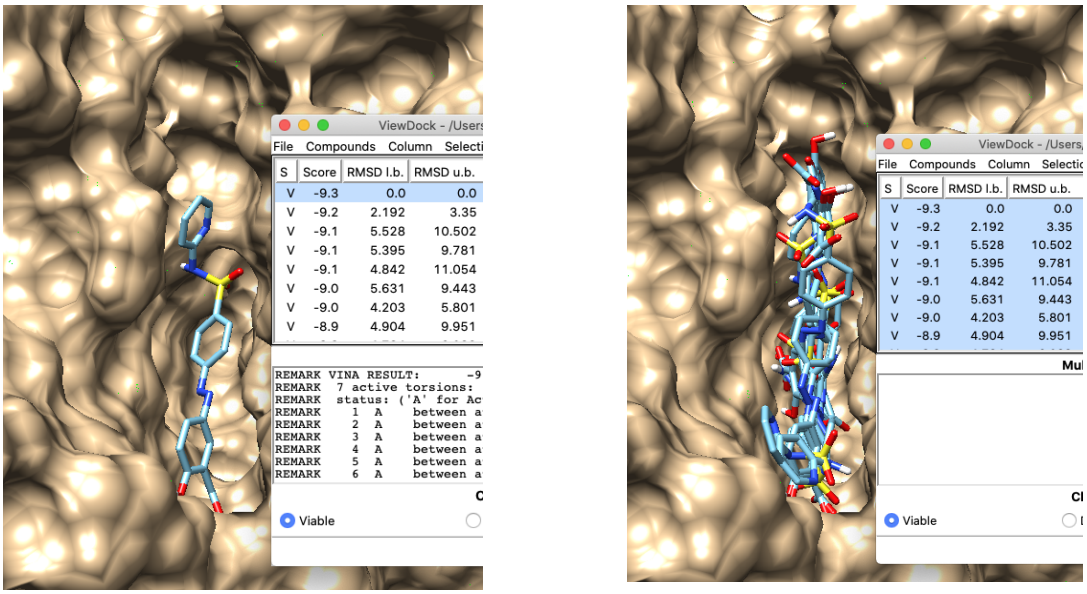

Figure 14. SFZ initial validation gives a Vina free energy score of -9.3 kcal/mol and matches the binding mode from the homology model in terms of the surrounding helices and residues.

4.6. Methods: Motivation for Further Design

The other known ligands, SB and ER, could be docked into the same binding pocket for even better binding scores, -9.8 kcal/mol and -11.1 kcal/mol respectively, lower than -9.3 kcal/mol, underscoring the possibility of further drug design.

A promising avenue to continue design after validation was differentiating the pharmacophores (substituents key to binding), innocuous auxophores (substituents innocuous to binding), and detrimental auxophores (substituents detrimental to binding) of each ligand. This would enable later substituent recombination, incorporating pharmacophores and avoiding auxophores.

4.7. Methods: Screening ZINC and PubChem

The differentiation could be done based on individually excising each substituent of a given ligand and considering the effect on binding performance, but instead, for greater accuracy and larger scale, I screened the ZINC and PubChem databases for similarity and substructure for the three known ligands SFZ, SB, and ER with a 40% threshold, yielding 1461 results.

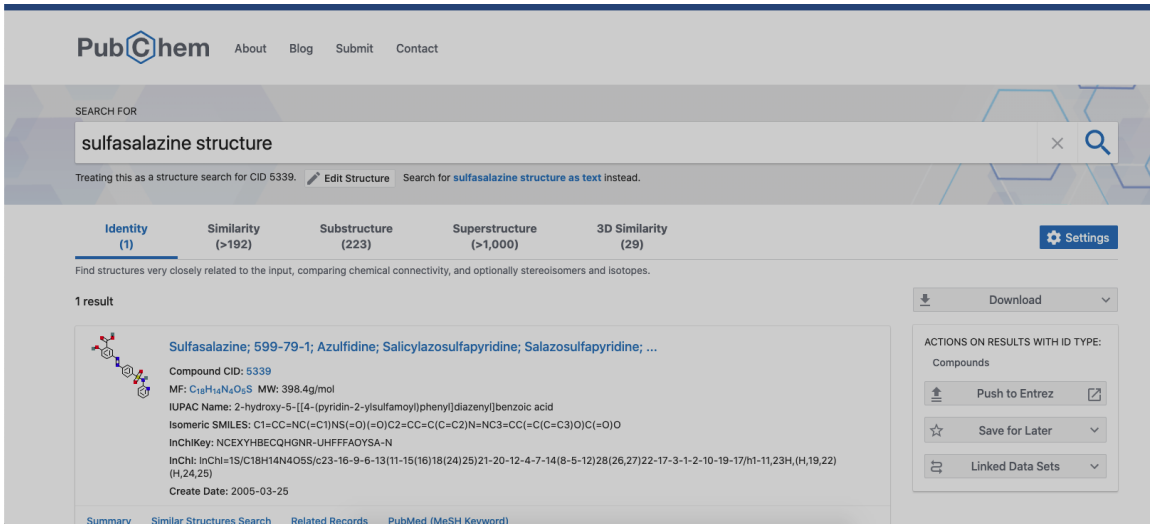

Figure 15. PubChem search for sulfasalazine, with tabs for similarity and substructure results.

Harnessing Bash scripting and Stony Brook's SeaWulf cluster, I docked all 1461 ligands in xCT's pocket and picked those with a binding score of -12 kcal/mol or better for further inspection. Consult the results for the two best screened ligands based on the multifaceted criteria established.

4.8. Methods: Substituent Recombination

Prior to screening, I also recombined substituents across the three known ligands to produce a multitude of recombinants. Most notably, because, in docking, SB was able to reach a portion near the top of the pocket that SFZ was unable to reach, I was motivated to add substituents from SB to SFZ. This portion near the top of the pocket was hydrophobic but polar with a positive electrostatic surface potential based on the hydrophobicity and Coulombic surfaces. Fluorine, the most electronegative element, is unique in that it is hydrophobic yet polar and δ-, so a substituent with fluorine was ideal for this part of the pocket. This motivated adding the CF3 substituent (which contains fluorine) from SB to the end of SFZ. I also tried both including and excluding the chlorobenzene ring right below it. Consult the results for the binding scores yielded.

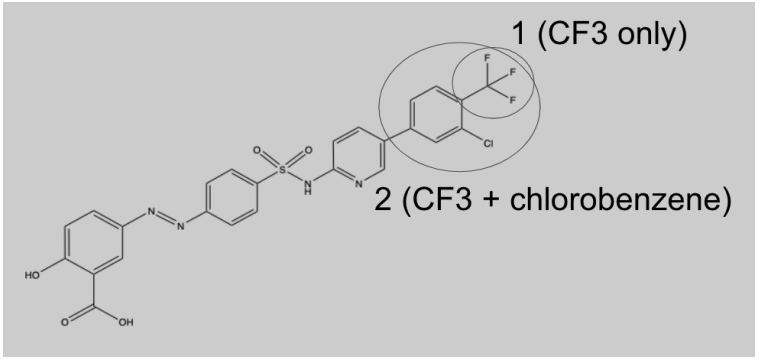

Figure 16. SFZ recombined with the CF3 and chlorobenzene substituents from SB.

5. Results and Conclusions

5.1. Results and Conclusions: Validation

In validation, I found that the key interacting amino acid residues in xCT's binding pocket were ARG135, GLN191, and LYS198, all of which formed hydrogen bonds for inhibition.

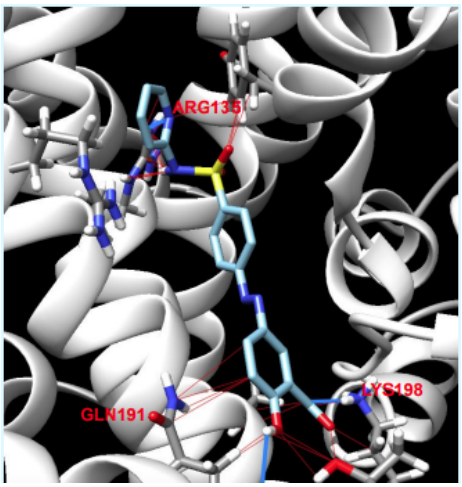

Figure 17. Key interacting hydrogen bonding residues for the initial validation of SFZ; the three are labeled and displayed in red above

5.2. Results and Conclusions: Substituent Recombination

Substituent recombination was tested for these amino acid residues by attaching CF3 and chlorobenzene substituents from SB to the end of SFZ to reach closer toward the top part of the pocket to increase inhibition because it has a positive electrostatic potential that complements fluorine's electronegativity. Then, I performed screening. The best binding score attained with recombinants prior to screening was -11.4.

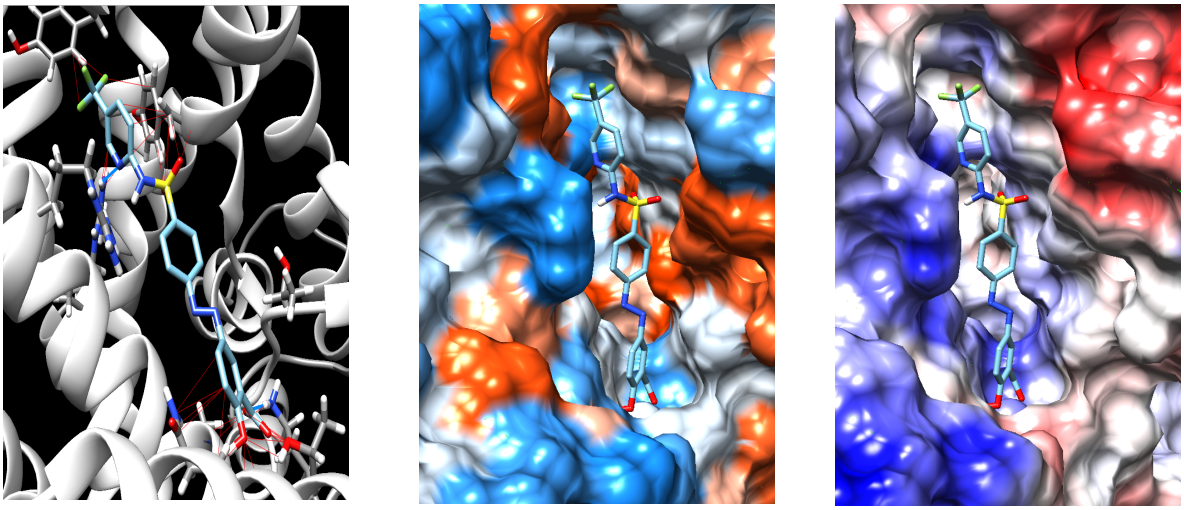

Figure 18. Interactions and Coulombic and hydrophobic surfaces of the SFZ + CF3 recombinant ligand. This yielded a significantly better docking score (-10.3 kcal/mol as opposed to -9.3 kcal/mol)

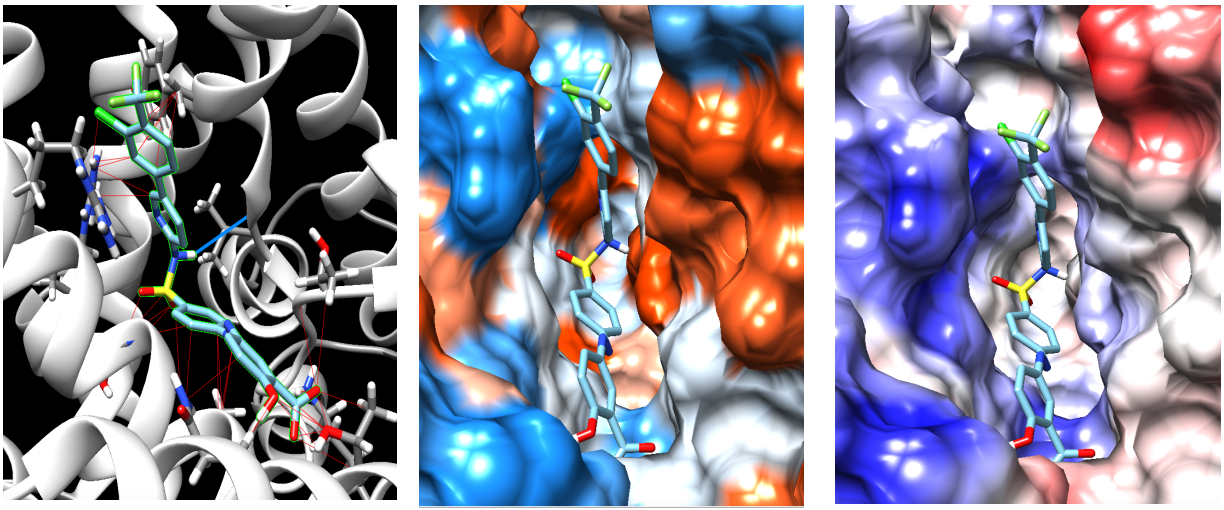

Figure 19. Interactions and Coulombic and hydrophobic surfaces of the SFZ + CF3 + chlorobenzene recombinant ligand. This yielded the best docking score among all recombinants (-11.4 kcal/mol as opposed to -9.3 kcal/mol).

5.3. Results and Conclusions: Screening

Screening for similarity and substructure yielded a total of 1461 results. The top two small molecule inhibitor drug candidates that can be used for the treatment of PDAC are below. Of the two, the latter has more hydrogen bonds and a LogP value less than 5, so it appears to be the best drug candidate. Furthermore, the change in Vina binding energy through drug design is -2.9 kcal/mol, so it is almost 138 times as potent as a drug candidate as the original SFZ molecule.

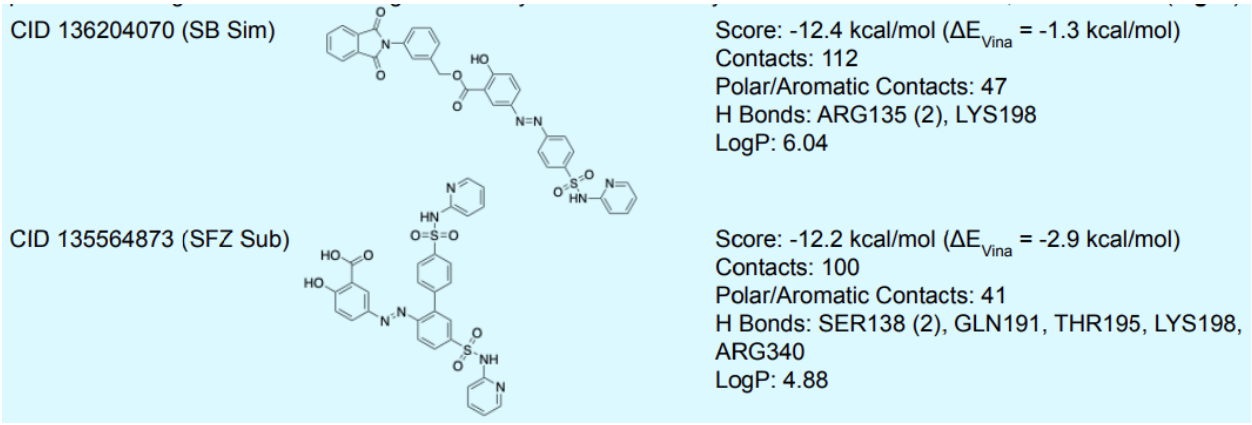

Figure 20. The top two small molecule drug candidates for PDAC, where the former is derived from a similarity search on SB and the latter is derived from a substructure search on SFZ. The latter, CID 135564873, is the best drug candidate out of all results.

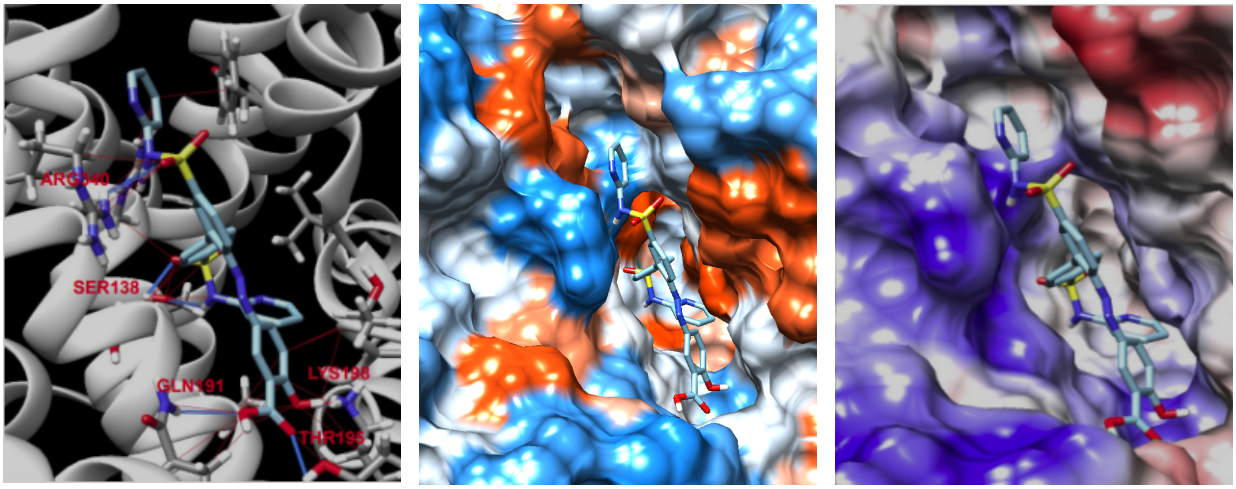

Figure 21. Interactions and Coulombic and hydrophobic surfaces for CID 135564873, the best drug candidate out of all results.

6. Acknowledgements

I would like to thank my mentor, Dr. Iwao Ojima, the Ojima group, the Simons Summer Research Program, and the Simons Foundation for giving me the opportunity to conduct this research.

7. References

(1) https://www.sciencedirect.com/topics/medicine-and-dentistry/docking-molecular (accessed Nov 10, 2021).

(2) Patel, D.; Kharkar, P. S.; Gandhi, N. S.; Kaur, E.; Dutt, S.; Nandave, M. Novel Analogs of Sulfasalazine as System Xc - Antiporter Inhibitors: Insights from the Molecular Modeling Studies. *Drug Dev. Res.* 2019, *80* (6), 758–777.

(3) Orth, M.; Metzger, P.; Gerum, S.; Mayerle, J.; Schneider, G.; Belka, C.; Schnurr, M.; Lauber, K. Pancreatic Ductal Adenocarcinoma: Biological Hallmarks, Current Status, and Future Perspectives of Combined Modality Treatment Approaches. *Radiat. Oncol.* 2019, *14* (1), 141.

(4) https://www.pancreaticcancer.org.uk/information/just-diagnosed-with-pancreatic-cancer/types-of-pancreatic-cancer/ (accessed Nov 10, 2021).

(5) von Ahrens, D.; Bhagat, T. D.; Nagrath, D.; Maitra, A.; Verma, A. The Role of Stromal Cancer-Associated Fibroblasts in Pancreatic Cancer. *J. Hematol. Oncol.* 2017, *10* (1). https://doi.org/10.1186/s13045-017-0448-5.

(6) Dongre, A.; Weinberg, R. A. New Insights into the Mechanisms of Epithelial-Mesenchymal Transition and Implications for Cancer. *Nat. Rev. Mol. Cell Biol.* 2019, *20* (2), 69–84.

(7) Koppula, P.; Zhuang, L.; Gan, B. Cystine Transporter SLC7A11/XCT in Cancer: Ferroptosis, Nutrient Dependency, and Cancer Therapy. *Protein Cell* 2021, *12* (8), 599–620.

(8) Habib, E.; Linher-Melville, K.; Lin, H. X.; Singh, G. Expression of XCT and Activity of System Xc() Are Regulated by NRF2 in Human Breast Cancer Cells in Response to Oxidative Stress. *Redox Biol* 2015, *5*, 33–42.

(9) Dixon, S. J.; Patel, D. N.; Welsch, M.; Skouta, R.; Lee, E. D.; Hayano, M.; Thomas, A. G.; Gleason, C. E.; Tatonetti, N. P.; Slusher, B. S.; Stockwell, B. R. Pharmacological Inhibition of Cystine-Glutamate Exchange Induces Endoplasmic Reticulum Stress and Ferroptosis. *Elife* 2014, *3*, e02523.

(10) Sontheimer, H.; Bridges, R. J. Sulfasalazine for Brain Cancer Fits. *Expert Opin. Investig. Drugs* 2012, *21* (5), 575–578.

(11) https://www.rcsb.org/structure/7CCS (accessed Nov 10, 2021).